LETTER

Protection against filovirus diseases by a novel broad–spectrum nucleoside analogue BCX4430

Travis K. Warren[1], Jay Wells[1], Rekha G. Panchal[1], Kelly S. Stuthman[1], Nicole L. Garza[1], Sean A. Van Tongeren[1], Lian Dong[1], Cary J. Retterer[1], Brett P. Eaton[1], Gianluca Pegoraro[1], Shelley Honnold[1], Shanta Bantia[2], Pravin Kotian[2], Xilin Chen[2], Brian R. Taubenheim[2]†, Lisa S. Welch[1], Dena M. Minning[3], Yarlagadda S. Babu[2], William P. Sheridan[2] & Sina Bavari[1]

Filoviruses are emerging pathogens and causative agents of viral haemorrhagic fever. Case fatality rates of filovirus disease outbreaks are among the highest reported for any human pathogen, exceeding 90% (ref. 1). Licensed therapeutic or vaccine products are not available to treat filovirus diseases. Candidate therapeutics previously shown to be efficacious in non-human primate disease models are based on virus-specific designs and have limited broad-spectrum antiviral potential. Here we show that BCX4430, a novel synthetic adenosine analogue, inhibits infection of distinct filoviruses in human cells. Biochemical, reporter-based and primer-extension assays indicate that BCX4430 inhibits viral RNA polymerase function, acting as a non-obligate RNA chain terminator. Post-exposure intramuscular administration of BCX4430 protects against Ebola virus and Marburg virus disease in rodent models. Most importantly, BCX4430 completely protects cynomolgus macaques from Marburg virus infection when administered as late as 48 hours after infection. In addition, BCX4430 exhibits broad-spectrum antiviral activity against numerous viruses, including bunyaviruses, arenaviruses, paramyxoviruses, coronaviruses and flaviviruses. This is the first report, to our knowledge, of non-human primate protection from filovirus disease by a synthetic drug-like small molecule. We provide additional pharmacological characterizations supporting the potential development of BCX4430 as a countermeasure against human filovirus diseases and other viral diseases representing major public health threats.

Members of the family *Filoviridae* include Ebola virus (EBOV), Marburg virus (MARV), Ravn virus (RAVV), Sudan virus (SUDV) and Bundibugyo virus (BDBV), all of which cause severe viral haemorrhagic fevers in humans. In nature, filoviruses are transmitted by physical contact between infected individuals, presumably via infected bodily fluids[2]. Initial filovirus disease manifestations include fever, headache, vomiting and diarrhoea[3]. Fatal cases are characterized by viraemia, elevated liver-associated enzyme levels, coagulopathy and haemorrhage. Filovirus disease outbreaks occur sporadically, most frequently in sub-Saharan Africa, with reported case fatality rates exceeding 90% (ref. 1). In 2012, simultaneous outbreaks involved MARV, SUDV and BDBV, an emergent filovirus isolated in 2007[4]. The historical occurrence of independent and simultaneous emergence of distinct filoviruses highlights the need for the identification and development of an efficacious broad-spectrum antiviral product.

Although no licensed antiviral preventative or therapeutic agents are currently available to combat filovirus disease in humans, a number of candidates are being developed and have been evaluated in non-human primate filovirus disease models. These models closely reproduce the known clinical and pathophysiological aspects of fatal human infection. Nucleic-acid-based products, antibody therapies and therapeutic vaccines have successfully protected non-human primates from filovirus disease[5–10], but these approaches rely on virus-specific designs that inherently limit the spectrum of activity and potential utility of individual treatments. The development of a single therapeutic agent active against multiple filoviruses would provide a key, cost-effective component of public-health preparedness plans in outbreak-prone regions.

The broad-spectrum antiviral agent ribavirin, a trizole nucleoside effective against multiple pathogenic RNA viruses, is not active against filoviruses[11]. Other small molecules—including the adenosine analogue 3-deazaneplanocin A (c[3]-Npc A) and T-705 (favipiravir), a substituted pyrazine compound —have conferred a high-degree of protection against filoviruses in rodents but have not been reported to protect non-human primates[12–18].

BCX4430, a novel nucleoside analogue (Fig. 1a), was synthesized (Supplementary Information) as part of a small-molecule library designed as inhibitors of viral RNA polymerase activity. BCX4430 is designed to inhibit viral RNA polymerase activity indirectly through non-obligate RNA chain termination, a mechanism requiring anabolism of the parent compound to BCX4430-triphosphate (BCX4430-TP). Then, after pyrophosphate cleavage, incorporation of BCX4430-monophosphate (BCX4430-MP) into nascent viral RNA strands would be expected to cause premature termination of transcription and replication of viral RNA. In support of this proposed mechanism, BCX4430 is rapidly phosphorylated to BCX4430-TP in cultured cell lines and primary hepatocytes, similar to the natural adenosine nucleoside (Fig. 1b and Extended Data Fig. 1a). Addition of BCX4430 reduces expression of green fluorescent protein (GFP) in an artificial EBOV minigenome replicon assay (Fig. 1c and Extended Data Fig. 1b), in which virion structural proteins comprising the viral ribonucleoprotein complex mediate transcription and replication of an RNA replicon template containing a GFP-reporter cassette. BCX4430-TP inhibits hepatitis C virus (HCV) RNA polymerase transcriptional activity in a cell-free, isolated enzyme transcription assay (Fig. 1d) (an isolated filovirus RNA polymerase enzyme assay has yet to be reported) and induces premature termination of RNA chain synthesis by HCV RNA polymerase during template-directed primer-extension assays (Fig. 1e and Extended Data Fig. 1c). In virus-infected cells, BCX4430 reduces surface-expressed MARV and EBOV glycoprotein and reduces the production of intracellular and extracellular MARV RNA (Fig. 1f–h and Extended Data Fig. 1d). Additionally, HeLa cells incubated with $\geq 25\,\mu M$ BCX4430 produce no detectable infectious MARV virus (concentration providing 90% inhibition (IC_{90}) = $5.4\,\mu M$) (Fig. 1h).

Taken together, these assessments strongly support our hypothesis that BCX4430 inhibits viral RNA polymerase function by inducing RNA chain termination. Findings from primer-extension reactions suggest that termination occurs two bases after incorporation of BCX4430-MP, perhaps as a result of inhibitory stereochemical distortions of the nascent RNA chain. We observed no evidence of BCX4430-MP incorporation into human RNA or DNA on exposing human Huh-7 cells to concentrations of BCX4430 exceeding the MARV IC_{50} by more than tenfold (Extended Data Fig. 1f). The basis of the selectivity of BCX4430 for viral polymerases is not yet known.

[1]Division of Molecular and Translational Sciences, Therapeutic Discovery Center, United States Army Medical Research Institute of Infectious Diseases (USAMRIID), Fort Detrick, Maryland 21702, USA. [2]BioCryst Pharmaceuticals Inc., Durham, North Carolina 27703, USA. [3]MedExpert Consulting, Inc., Indialantic, Florida 32903, USA. †Present address: Wilco Consulting, LLC, Durham, North Carolina 27712, USA.
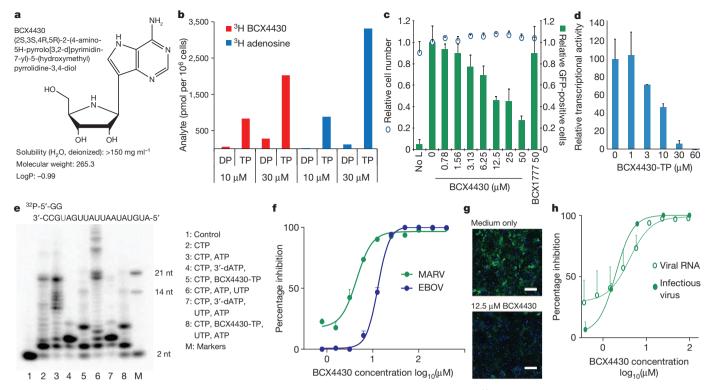
Figure 1 | Pharmacological characterization of BCX4430. a, BCX4430 chemical structure and properties. LogP, log of partition coefficient. **b**, Conversion of ^{3}H-BCX4430 or ^{3}H-adenosine to diphosphate (DP) or triphosphate (TP) forms in Huh-7 cells ($n = 1$). **c**, Effect of BCX4430 on replication of an EBOV minigenome RNA replicon in cultured cells ($n = 6$). No L, L-polymerase encoding plasmid omitted from reaction. **d**, BCX4430-TP suppresses HCV NS5B (NS5B-1b-Δ21) RNA polymerase activity ($n = 2$). **e**, RNA products synthesized by purified HCV polymerase, in a template-directed primer (^{32}P-5'-GG) extension assay. nt, nucleotides. **f**, Expression of EBOV and MARV glycoprotein in infected HeLa cells ($n = 5$–6). **g**, MARV-infected HeLa cells. Green, α-MARV glycoprotein; blue, Hoechst dye. Scale bar, 100 μm. **h**, Production of intracellular MARV RNA ($n = 4$) and infectious virus in MARV-infected HeLa cells ($n = 2$ technical replicates). Data in **c**, **d**, and **h** are expressed as mean + standard deviation (s.d.). Data in **f** are expressed as mean + standard error of the mean (s.e.m.).

To assess the spectrum of antiviral activity of BCX4430, we conducted additional high-content image (HCI)-based and neutral-red uptake antiviral assays using an array of other human viruses. BCX4430 exhibited antiviral activity against negative-sense RNA viruses representing the *Filoviridae*, *Arenaviridae*, *Bunyaviridae*, *Orthomyxoviridae*, *Picornaviridae* and *Paramyxoviridae* families, and positive-sense RNA viruses of the *Flaviviridae* and *Coronaviridae* families (Table 1 and Extended Data Fig. 2). Antiviral effects were specific and did not result from cellular toxicity or anti-proliferative effects, as assessed by enumeration of live cells during all HCI assays and by the lactate dehydrogenase (LDH) release assay. In HeLa cells, the 50% cytotoxic concentration (CC$_{50}$) of BCX4430 exceeded 500 μM as determined by the LDH assay, and consistently exceeded 100 μM using the HCI-based assay (Table 1). An antiviral effect was confirmed in infected human macrophages cultured from normal peripheral blood monocytes, using EBOV (Extended Data Fig. 1e). It is important to note that immortalized cell lines exhibit a substantially attenuated capacity to convert BCX4430 to its active TP form, compared with primary hepatocytes (Extended Data Fig. 1a). Thus, the results obtained from antiviral assessments relying on immortalized cells may underrepresent the antiviral potency of BCX4430 achievable *in vivo* during experimental or clinical infections.

In preparation for *in vivo* pharmacokinetics and efficacy testing, we sought to further characterize potential adverse pharmacological features of BCX4430 that could limit its utility *in vivo* or clinically. BCX4430 exhibited no mutagenicity when tested using the Ames assay at 5 mg per plate, produced no detectable chromosomal aberrations in human lymphocytes at a concentration of 787 μM, and did not inhibit the hERG ion channel current at 30 μM (data not shown). The compound is metabolically stable (half-life ($t_{1/2}$) > 54 min) when incubated with S9 liver fractions obtained from various animal species (Extended Data Table 1).

In mouse, rat, guinea pig and cynomolgus macaque, BCX4430 pharmacokinetics were characterized by rapid clearance from the plasma with a half-life of <5 min (Fig. 2b, Extended Data Fig. 4c and Extended

Table 1 | BCX4430 antiviral activity

Virus family	Virus	Strain/variant	EC$_{50}$ (μM)	EC$_{90}$ (μM)	CC$_{50}$ (μM)
Filoviridae	MARV	Musoke*	4.4	10.5	242
	MARV	Ci67*	6.7	16.1	255
	MARV	Angola*	5.0	12.3	242
	EBOV	Kikwit*	11.8	25.4	>100
	SUDV	Boniface*	3.4	10.3	>100
Togaviridae	VEEV	SH3*	>100	>100	>100
	EEEV	FL93-939†	43.2	>100	>100
	WEEV	California†	21.3	>30	>100
	CHIKV	AF 15561*	>100	>100	>100
Bunyaviridae	RVFV	ZH5018*	41.6	98.0	>100
	LACV	Wisconsin 1960†	13.4	65.0	>100
	MPRLV	HV97021050†	40.1	95.0	>250
Arenaviridae	LASV	Josiah*	43.0	>100	>100
	JUNV	Romero*	42.2	>100	>100
Paramyxoviridae	NiV	Malaysia*	41.9	>100	>100
	RSV	2305†	11.0	25.7	>89
	MeV	Chicago†	6.19	34.4	>296
Coronaviridae	MERS-CoV	Jordan N3*	68.4	>100	>100
	SARS-CoV	Urbani†	57.7	>95	>296
Orthomyxoviridae	Influenza	pH1N1†	10.7	17.0	>296
Picornaviridae	HRV2	HGP†	3.4	45.2	>296
Flaviviridae	YFV	17D†	14.1	46.8	>100
	JEV	SA14†	43.6	93.4	>100
	DENV2	New Guinea C†	32.8	89.3	>296

EC$_{50}$, 50% effective concentration; EC$_{90}$, 90% effective concentration. Definitions for virus abbreviations are provided in Methods.
* Antiviral activity assessed by high-content image analysis.
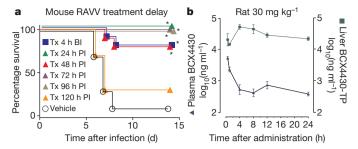† Antiviral activity assessed by neutral-red uptake assay.

Figure 2 | BCX4430 *in vivo* efficacy and pharmacokinetics characterization. a, Survival of RAVV-infected mice ($n = 9$–10 per group). BCX4430 treatments (Tx) were administered i.m. twice daily at 150 mg kg^{-1} doses for 9 days beginning at the indicated time before infection (BI) or post-infection (PI). **b,** Pharmacokinetics of BCX4430 and BCX4430-TP in Sprague–Dawley rats ($n = 3$) after single-dose i.m. administration of BCX4430. *$P < 0.05$ treatment versus vehicle survival curves by log-rank (Mantel–Cox) test. Data in **b** are expressed as mean ± s.e.m.

Data Table 2). By contrast, the half-life of the active BCX4430-TP form in the liver in rats was substantially longer at 6.2 h (Fig. 2b).

Rodent models of filovirus disease do not always reliably reproduce the pathophysiology observed in humans and non-human primates. Nevertheless, rodent systems can provide proof-of-concept efficacy and inform dose and treatment-regimen selection for non-human primate efficacy trials. In RAVV-infected mice, intramuscular (i.m.) administration of BCX4430 conferred a high degree of protection (75–100%) in groups treated prophylactically at doses ≥3.3 mg kg^{-1} (Extended Data Fig. 3a, b). Notably, significant protection ($P < 0.05$) was also observed with doses of 150 mg kg^{-1} initiated at times as long as 96 h after infection (Fig. 2a). Additionally, we demonstrated that mice administered BCX4430 either i.m. or orally were protected against lethal EBOV challenge and that mice receiving i.m. treatments were protected against lethal Rift Valley fever virus challenge (Extended Data Fig. 3c, d).

The *in vivo* post-exposure efficacy of BCX4430 was further verified in two guinea pig models of MARV disease[19] in which animals were challenged either by intraperitoneal (i.p.) injection, or, because filoviruses can be transmitted via aerosolized particles[20], by exposure to aerosolized virus. In both the i.p. and aerosolized-virus challenge models, BCX4430 conferred significant post-exposure protection when treatment was initiated within 48 h of virus exposure (Extended Data Fig. 4a). In the respiratory exposure model, BCX4430 protected guinea pigs when treatment initiation was delayed to 72 h after infection, the longest delay tested (Extended Data Fig. 4b).

We further explored the post-exposure efficacy of BCX4430 using the cynomolgus macaque MARV disease model, which accurately reproduces filovirus disease manifestations observed in fatal human cases[21]. Cynomolgus macaques were experimentally infected with a lethal dose of wild-type MARV (Musoke variant), derived from a human clinical isolate[22], and animals were administered with 15 mg kg^{-1} BCX4430 twice daily by i.m. injection beginning 1–48 h after infection and continuing for 14 days. The six infection-control subjects succumbed by day 12 (Fig. 3a), after having developed viraemia (Fig. 3b) and characteristic signs of filovirus disease, including behavioural inactivity, maculopapular rash, increases in liver injury markers such as aspartate aminotransferase and bilirubin (Fig. 3c, d), and prolongations of prothrombin time (PT) and activated partial thromboplastin time (aPTT) (Fig. 3e, f). All animals treated with BCX4430 beginning 24 or 48 h after infection survived. Five out of six (83%) animals treated with BCX4430 beginning 1 h after infection survived (Fig. 3a). Consistent with the proposed antiviral mechanism of action, BCX4430 significantly and substantially reduced serum MARV burden (Fig. 3b), without inducing type I interferon responses (Extended Data Fig. 4d), as has been observed for c^3-Npc A in mice[15]. Additionally, BCX4430 ameliorated haemorrhagic disease manifestations, as evidenced by shorter PT and aPTT times and reduced laboratory
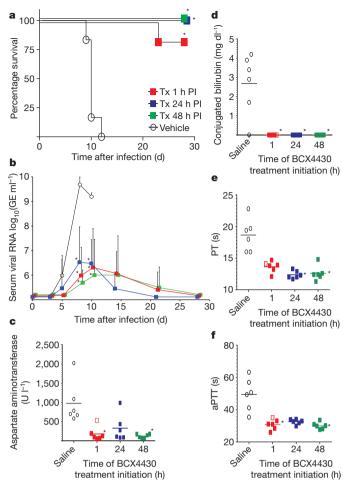

Figure 3 | Post-exposure protection of MARV-infected cynomolgus macaques by BCX4430. a–f, Animals ($n = 6$) were challenged with MARV by subcutaneous injection, and BCX4430 (Tx) (15 mg kg^{-1} twice daily) or vehicle was administered i.m. beginning at the indicated times after challenge. **a,** Kaplan–Meier survival curves. PI, post-infection. **b,** Serum viral RNA load. GE, genomic equivalents. **c–f,** Individual animal maximal values of serum aspartate aminotransferase concentrations (**c**), conjugated bilirubin concentrations (**d**), PT (**e**) and aPTT (**f**). Non-survivors are represented by open symbols. *$P < 0.05$ for comparison of treatment versus vehicle by log-rank (Mantel–Cox) test (**a**), two-tailed analyses using the Holm–Sidak method (**b**), or two-tailed Kruskal–Wallis test followed by Dunn's post-test comparison (**c–f**). Data in **b** are expressed as geometric mean + s.d. Horizontal bars in **c–f** represent group means.

indices of liver damage, such as serum AST and bilirubin concentrations, compared with vehicle treatment (Fig. 3c–f).

Outbreaks in 2012 involving MARV, SUDV and BDBV reported in Uganda and the Democratic Republic of the Congo highlight the urgent need for development of an effective antiviral product to counter filovirus disease. For the first time, to our knowledge, we report the identification of a small molecule with efficacy against filovirus disease in non-human primates. Furthermore, we have provided evidence that BCX4430 exhibits broad-spectrum antiviral activity against other highly virulent RNA viruses (Table 1 and Extended Data Fig. 2). Additional evaluations are in progress to assess the *in vivo* efficacy of BCX4430 against EBOV and other highly virulent pathogens in non-human primates or other disease models that most closely recapitulate human disease.

BCX4430 was well tolerated, producing no overt signs of systemic toxicity or adverse local reactions in any of the efficacy studies. The substantial efficacy of BCX4430 observed with the i.m. route, which provides high bioavailability and rapid absorption, is conducive for use during outbreaks, potentially enabling administration by individuals lacking advanced medical training. In MARV-infected cynomolgus macaques,

we did not observe any diminution of protective effects with delay of BCX4430 treatment initiation up to 48 h after infection, suggesting that even greater delays of treatment, yet to be tested, may also yield significant protective benefit. In preparation for advancing BCX4430 into human phase 1 clinical trials in the United States, additional studies are in progress to support filing of an Investigational New Drug Application.

METHODS SUMMARY

BCX4430 was synthesized by BioCryst Pharmaceuticals. Cell-based infection assays were conducted using HCI-based analyses as described previously[23] for filoviruses and Rift Valley fever virus. For other viruses, inhibition of virus-induced cytopathic effect (CPE) was assessed in cell-based assays using neutral-red uptake, as described previously[24]. Replication of EBOV minigenome RNA constructs was assayed by using a plasmid-based reconstituted replication/transcription system[25]. Inhibition of RNA transcriptional activity was assessed in an isolated HCV polymerase assay[26] and inhibition of HCV polymerase RNA synthesis activity was evaluated using a template-driven ^{32}P-GG primer extension assay. Mouse models of EBOV, MARV and RAVV disease have been described previously[27,28]. Experiments were conducted using mouse-adapted strains of EBOV (Mayinga variant) and RAVV (Ravn variant). A guinea pig MARV-Musoke parenteral challenge model and virus aerosolization methods used for guinea pig exposures have been previously described[19,29]. BCX4430 was administered in a vehicle of sterile 0.9% saline for injection for all *in vivo* applications. Animal infection experiments were performed in biosafety level 4 containment facilities at the United States Army Medical Research Institute of Infectious Diseases (USAMRIID). All experimental treatment replication was conducted using biological replication, except for the virus-yield reduction assay (Fig. 1h), which relied on technical replication.

Research was conducted under an Institutional Animal Care and Use Committee approved protocol in compliance with the Animal Welfare Act, PHS Policy and other federal statutes and regulations relating to animals and experiments involving animals. The facility where this research was conducted is accredited by the Association for Assessment and Accreditation of Laboratory Animal Care, International and adheres to principles stated in the Guide for the Care and Use of Laboratory Animals, National Research Council, 2011.

1. Kuhn, J. H. *Filoviruses: A Compendium of 40 Years of Epidemiological, Clinical, and Laboratory Studies* (Springer, 2008).
2. Bausch, D. G. *et al.* Assessment of the risk of Ebola virus transmission from bodily fluids and fomites. *J. Infect. Dis.* **196** (suppl. 2), S142–S147 (2007).
3. Kortepeter, M. G., Bausch, D. G. & Bray, M. Basic clinical and laboratory features of filoviral hemorrhagic fever. *J. Infect. Dis.* **204** (suppl. 3), S810–S816 (2011).
4. Towner, J. S. *et al.* Newly discovered Ebola virus associated with hemorrhagic fever outbreak in Uganda. *PLoS Pathog.* **4**, e1000212 (2008).
5. Geisbert, T. W. *et al.* Vesicular stomatitis virus-based vaccines protect nonhuman primates against aerosol challenge with Ebola and Marburg viruses. *Vaccine* **26**, 6894–6900 (2008).
6. Geisbert, T. W. *et al.* Postexposure protection of non-human primates against a lethal Ebola virus challenge with RNA interference: a proof-of-concept study. *Lancet* **375**, 1896–1905 (2010).
7. Warfield, K. L. *et al.* Ebola virus-like particle-based vaccine protects nonhuman primates against lethal Ebola virus challenge. *J. Infect. Dis.* **196** (suppl. 2), S430–S437 (2007).
8. Warren, T. K. *et al.* Advanced antisense therapies for postexposure protection against lethal filovirus infections. *Nature Med.* **16**, 991–994 (2010).
9. Dye, J. M. *et al.* Postexposure antibody prophylaxis protects nonhuman primates from filovirus disease. *Proc. Natl Acad. Sci. USA* **109**, 5034–5039 (2012).
10. Sullivan, N. J., Sanchez, A., Rollin, P. E., Yang, Z. Y. & Nabel, G. J. Development of a preventive vaccine for Ebola virus infection in primates. *Nature* **408**, 605–609 (2000).
11. Huggins, J. W. Prospects for treatment of viral hemorrhagic fevers with ribavirin, a broad-spectrum antiviral drug. *Rev. Infect. Dis.* **11** (suppl. 4), S750–S761 (1989).
12. Smither, S. J. *et al.* Post-exposure efficacy of Oral T-705 (Favipiravir) against inhalational Ebola virus infection in a mouse model. *Antiviral Res.* http://dx.doi.org/10.1016/j.antiviral.2014.01.012 (2014).
13. Aman, M. J. *et al.* Development of a broad-spectrum antiviral with activity against Ebola virus. *Antiviral Res.* **83**, 245–251 (2009).
14. Bray, M., Driscoll, J. & Huggins, J. W. Treatment of lethal Ebola virus infection in mice with a single dose of an *S*-adenosyl-L-homocysteine hydrolase inhibitor. *Antiviral Res.* **45**, 135–147 (2000).
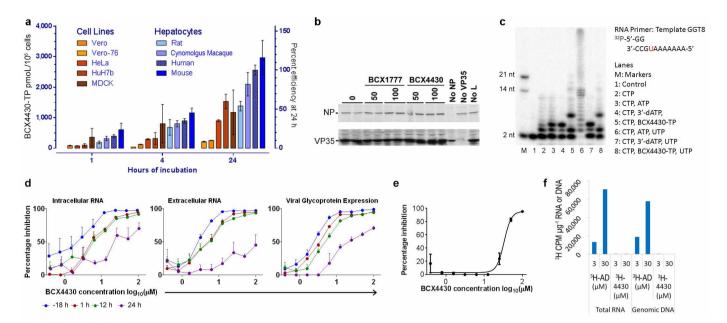15. Bray, M., Raymond, J. L., Geisbert, T. & Baker, R. O. 3-Deazaneplanocin A induces massively increased interferon-α production in Ebola virus-infected mice. *Antiviral Res.* **55**, 151–159 (2002).
16. Kinch, M. S. *et al.* FGI-104: a broad-spectrum small molecule inhibitor of viral infection. *Am. J. Transl. Res.* **1**, 87–98 (2009).
17. Panchal, R. G. *et al.* Identification of an antioxidant small-molecule with broad-spectrum antiviral activity. *Antiviral Res.* **93**, 23–29 (2012).
18. Warren, T. K. *et al.* Antiviral activity of a small-molecule inhibitor of filovirus infection. *Antimicrob. Agents Chemother.* **54**, 2152–2159 (2010).
19. Hevey, M., Negley, D., Pushko, P., Smith, J. & Schmaljohn, A. Marburg virus vaccines based upon alphavirus replicons protect guinea pigs and nonhuman primates. *Virology* **251**, 28–37 (1998).
20. Kobinger, G. P. *et al.* Replication, pathogenicity, shedding, and transmission of Zaire ebolavirus in pigs. *J. Infect. Dis.* **204**, 200–208 (2011).
21. Bente, D., Gren, J., Strong, J. E. & Feldmann, H. Disease modeling for Ebola and Marburg viruses. *Dis. Model. Mech.* **2**, 12–17 (2009).
22. Smith, D. H. *et al.* Marburg-virus disease in Kenya. *Lancet* **319**, 816–820 (1982).
23. Panchal, R. G. *et al.* Development of high-content imaging assays for lethal viral pathogens. *J. Biomol. Screen.* **15**, 755–765 (2010).
24. Barnard, D. L. *et al.* Inhibition of measles virus replication by 5′-nor carbocyclic adenosine analogues. *Antivir. Chem. Chemother.* **12**, 241–250 (2001).
25. Mühlberger, E., Weik, M., Volchkov, V. E., Klenk, H. D. & Becker, S. Comparison of the transcription and replication strategies of Marburg virus and Ebola virus by using artificial replication systems. *J. Virol.* **73**, 2333–2342 (1999).
26. Lou, H., Choi, Y. H., LaVoy, J. E., Major, M. E. & Hagedorn, C. H. Analysis of mutant NS5B proteins encoded by isolates from chimpanzees chronically infected following clonal HCV RNA inoculation. *Virology* **317**, 65–72 (2003).
27. Bray, M., Davis, K., Geisbert, T., Schmaljohn, C. & Huggins, J. A mouse model for evaluation of prophylaxis and therapy of Ebola hemorrhagic fever. *J. Infect. Dis.* **178**, 651–661 (1998).
28. Warfield, K. L. *et al.* Development and characterization of a mouse model for Marburg hemorrhagic fever. *J. Virol.* **83**, 6404–6415 (2009).
29. Alves, D. A. *et al.* Aerosol exposure to the Angola strain of Marburg virus causes lethal viral hemorrhagic fever in cynomolgus macaques. *Vet. Pathol.* **47**, 831–851 (2010).
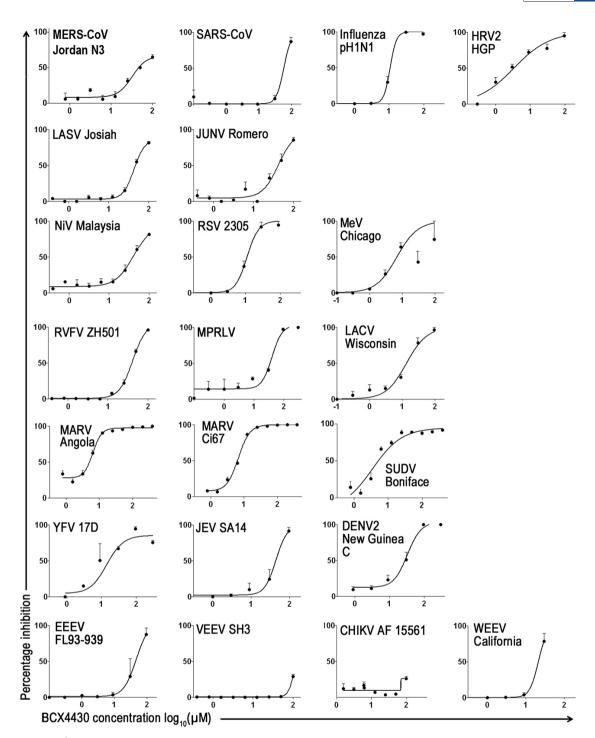
Author Contributions Y.S.B. and P.K. were responsible for the synthesis of BCX4430 and other small molecules. T.K.W. designed and supervised activities associated with rodent and non-human primate efficacy evaluations, evaluated study results, and wrote the manuscript. J.W., K.S.D., N.L.G. and S.A.V.T. conducted the rodent and non-human primate efficacy studies and performed sample analyses. R.G.P., G.P., C.J.R. and B.P.E. designed and executed cell-based filovirus assays and analysed these data. S. Bantia, Y.S.B., D.M.M., W.P.S., B.R.T. and others designed and analysed data from cell-based antiviral assays. L.D. conducted quantitative PCR analysis. B.R.T. conducted statistical evaluations of *in vivo* study results. S.H. performed post-mortem analysis of all non-human primate subjects. Y.S.B. supervised the pharmacokinetics studies of BCX4430 and W.P.S. conducted pharmacokinetics data analysis. S. Bantia conducted assessments of BCX4430 metabolite analysis and incorporation into host nucleic acids. X.C. conducted chain termination experiments. T.K.W., D.M.M., L.S.W., B.R.T., Y.S.B., W.P.S. and S. Bavari designed experiments, evaluated results and provided project oversight.

Author Information Reprints and permissions information is available at www.nature.com/reprints. The authors declare competing financial interests: details are available in the online version of the paper. Readers are welcome to comment on the online version of the paper. Correspondence and requests for materials should be addressed to S. Bavari (sina.bavari.civ@mail.mil).
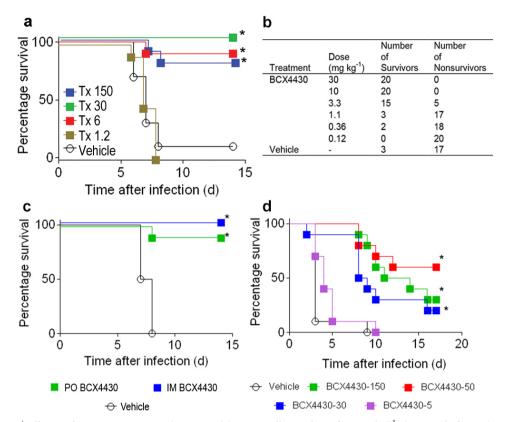
Extended Data Figure 1 | Phosphorylation and antiviral mechanism of action of BCX4430. a, Conversion of BCX4430 to the active triphosphate (TP) form in cultured cell lines and fresh primary hepatocytes ($n = 3$–6). Right axis, values normalized to mean 24 h value for human hepatocytes. **b**, Expression of EBOV NP and VP35 in an EBOV minigenome RNA replicon assay, in BHK-21-derived cells ($n = 6$). Right three lanes, plasmids expressing the indicated viral protein were omitted from the transfection mix. Gel image cropped for clarity. **c**, RNA products synthesized by purified HCV polymerase, in a template-directed primer (^{32}P-5′-GG) extension assay. **d**, Production of intra- and extracellular MARV RNA and cell-surface expression of viral glycoprotein in MARV-infected HeLa cells ($n = 4$) treated with BCX4430 either 18 h before infection, or 1, 12 or 24 h after infection. **e**, Expression of EBOV glycoprotein in monocyte-derived primary human macrophages ($n = 4$). **f**, Incorporation of ^{3}H-BCX4430 (^{3}H-4430) or ^{3}H-adenosine (^{3}H-AD) in human Huh-7 cells after 24 h incubation ($n = 1$). CPM, counts per min. Percentage inhibition assessed against the average of medium-only infection-control wells. Data in **a** are expressed as mean ± s.d. Data in **d** are expressed as mean + s.e.m. Data in **e** are expressed as mean ± s.e.m.
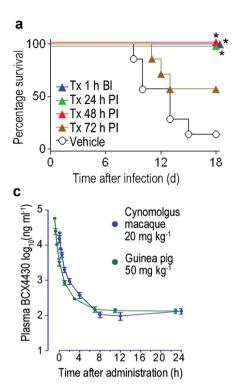
Extended Data Figure 2 | Broad-spectrum antiviral activity of BCX4430. Antiviral activity was assessed in cell-based assays ($n = 3$–5; $n = 2$, MERS-CoV), either using high-content image-based analysis or neutral-red uptake, using cell lines described in Methods. Cells were pre-treated with BCX4430 for ~18 h before infection. Definitions of virus abbreviations are provided in Methods. Except for the top row, viruses are arranged in rows by taxonomic family. Percentage inhibition of BCX4430-treatment wells was assessed against the average of medium-only infection-control wells. Negative inhibition values were transformed to zero for curve fit analysis and display. Data are expressed as mean + s.e.m.
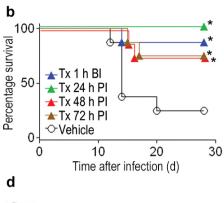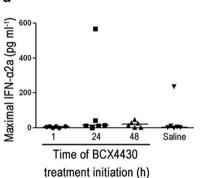
Extended Data Figure 3 | Efficacy of BCX4430 in mouse disease models.
a, **b**, BCX4430 dose versus survival of RAVV-infected mice (**a**, $n = 9$–10).
BCX4430 treatments (Tx) were administered for 9 days beginning ~4 h before
infection. Numbers in panel **a** indicate mg kg^{-1} doses. **c**, Survival of mice
($n = 10$) infected with EBOV. BCX4430 was administered twice daily i.m. or
orally at a dose of 150 mg kg^{-1}. **d**, Survival of mice ($n = 10$) infected with
RVFV. BCX4430 was administered twice daily at doses of 5–150 mg kg^{-1} by
i.m. injection. *$P < 0.05$ for comparison of treatment versus vehicle survival
curves by log-rank (Mantel–Cox) test.

Extended Data Figure 4 │ *In vivo* activity of BCX4430 in guinea pigs and cynomolgus macaques. **a**, **b**, Survival of guinea pigs ($n = 8$ per group) infected by i.p. injection with MARV-Musoke (**a**) or by exposure to aerosolized MARV-Angola (**b**). BCX4430 (i.m., 50 mg kg^{-1} twice daily) treatments (Tx) began at the indicated times before infection (BI) or post-infection (PI). **c**, Pharmacokinetics of BCX4430 in guinea pigs and cynomolgus macaques ($n = 3$) after single-dose i.m. administration. **d**, Individual animal maximal values of interferon-α2a in MARV-infected cynomolgus macaques. *$P < 0.05$ for comparison of treatment versus vehicle survival curves by log-rank (Mantel–Cox) test. Data in **c** are expressed as mean ± s.e.m. Horizontal bars in **d** represent group means.

Extended Data Table 1 │ *In vitro* metabolic stability of BCX4430 in liver S9 fractions

Species	% Remaining of Initial (n=1)[*]					Half-life[†] (min)	CL_{int}[‡] (mL/min/mg protein)	Metabolites Detected[§]
	0 min	10 min	20 min	30 min	60 min			
Rat	100	84.7	84.7	74.6	86.7	> 60	0.0021	No
Dog	100	87.6	89.1	79.2	54.6	> 60	0.0092	No
Human	100	91.8	81.7	71.1	45.1	54.2	0.0128	No
Monkey	100	84.4	88.9	89.9	69.4	> 60	0.0050	No
Mouse	100	78.0	89.2	75.6	57.1	> 60	0.0084	No

* Percentage remaining of test compound was calculated based on the peak area ratio of the test compound to the internal standard by LC-HRMS. Performance of positive biocontrol reagents testosterone and 7-hydroxycoumarin was assessed in parallel and met assay acceptability specifications.
† Half-life was calculated as $t_{1/2} = 0.693/k$, where k is the elimination rate constant in the equation describing first-order decay ($C_t = C_0 \times e^{-kt}$), and C_t and C_0 are the peak area ratios at time t and time 0, respectively. Data points were fitted to a first-order decay model by nonlinear regression, using GraphPad Prism (version 5.04 or higher) without weighting or any user intervention.
‡ Intrinsic clearance (CL_{int}) was calculated based on $CL_{int} = k/P$, where k is the elimination rate constant and P is the protein concentration in the incubation.
§ Expected metabolite(s) detected.

Extended Data Table 2 | BCX4430 and BCX4430-TP pharmacokinetics

Species	Dose (mg kg^{-1})	Route	C_{max} ng mL^{-1} (plasma) ng g^{-1} (liver)	T_{max}	AUC ng×hr mL^{-1} (plasma) ng×hr g^{-1} (liver)	AUC adjusted for dose administered	$T_{1/2\alpha}$
Plasma PK parameters for BCX4430							
Cynomolgus macaque	20	IM	22,333	5 min	13,109	655	10.1 min
Guinea pig	50	IM	56,333	5 min	20,545	411	5.6 min
Rat	2	IV	6,890	5 min	1,070	535	1.9 min
Mouse	2	IV	2,943	5 min	619	310	1.9 min
Liver PK parameters for BCX4430-TP							
Rat	30	IM	53,511	4 h	766,982	25,566	6.2 h
Mouse	150	IM	320,695	8 h	4,566,000	30,373	4.3 h

Pharmacokinetics parameters were calculated from plasma BCX4430 and liver BCX4430-TP levels. Liver BCX4430-TP C_{max} and area under the curve (AUC) parameters are expressed in parent drug equivalents.